

Article

Various Oxygen-Centered Phosphanegold(I) Cluster Cations Formed by Polyoxometalate (POM)-Mediated Clusterization: Effects of POMs and Phosphanes

Takuya Yoshida ^{1,2,3}, Yuta Yasuda ¹, Eri Nagashima ¹, Hidekazu Arai ¹, Satoshi Matsunaga ¹ and Kenji Nomiya ^{1,*}

¹ Department of Chemistry, Faculty of Science, Kanagawa University, Tsuchiya 2946, Hiratsuka, Kanagawa 259-1293, Japan; E-Mails: tyoshida@tmu.ac.jp (T.Y.);

yuy_inorg_chem@yahoo.co.jp (Y.Y.); r201470053hb@kanagawa-u.ac.jp (E.N.);

r201470040ur@kanagawa-u.ac.jp (H.A.); matsunaga@kanagawa-u.ac.jp (S.M.)

² Research Center for Gold Chemistry, Graduate School of Urban Environmental Sciences, Tokyo Metropolitan University, 1-1 Minami-osawa, Hachioji, Tokyo 192-0397, Japan

³ Department of Applied Chemistry, Graduate School of Urban Environmental Sciences, Tokyo Metropolitan University, 1-1 Minami-osawa, Hachioji, Tokyo 192-0397, Japan

* Author to whom correspondence should be addressed; E-Mail: nomiya@kanagawa-u.ac.jp; Tel.: +81-463-59-4111; Fax: +81-463-58-9684.

External Editor: Ahmed A. Mohamed

Received: 13 October 2014; in revised form: 13 November 2014 / Accepted: 14 November 2014 /

Published: 10 December 2014

Abstract: Novel phosphanegold(I) cluster cations combined with polyoxometalate (POM) anions, *i.e.*, intercluster compounds, [(Au{P(*m*-FPh)₃})₄(μ₄-O)]₂[(Au{P(*m*-FPh)₃})₂(μ-OH)]₂[α-PMo₁₂O₄₀]₂·EtOH (**1**), [(Au{P(*m*-FPh)₃})₄(μ₄-O)]₂[α-SiMo₁₂O₄₀]₂·4H₂O (**2**), [(Au{P(*m*-MePh)₃})₄(μ₄-O)]₂[α-SiM₁₂O₄₀] (*M* = W (**3**), Mo (**4**)) and [(Au{P(*p*-MePh)₃})₄(μ₄-O)]₂[(Au{P(*p*-MePh)₃})₃(μ₃-O)]₂[α-PW₁₂O₄₀] (**5**) were synthesized by POM-mediated clusterization, and unequivocally characterized by elemental analysis, TG/DTA, FT-IR, X-ray crystallography, solid-state CPMAS ³¹P NMR and solution (¹H, ³¹P{¹H}) NMR. Formation of these gold(I) cluster cations was strongly dependent upon the charge density and acidity of the POMs, and the substituents and substituted positions on the aryl group of triarylphosphane ligands. These gold(I) cluster cations contained various bridged-oxygen atoms such as μ₄-O, μ₃-O and μ-OH groups.

Keywords: phosphanegold(I) cluster; polyoxometalate; oxygen-center; intercluster compound

1. Introduction

Polyoxometalates (POMs) are discrete metal oxide clusters that are of current interest as soluble metal oxides and for their applications in catalysis, medicine and materials science [1–6]. The preparation of POM-based materials is therefore an active field of research. One of the intriguing aspects of POMs is that their combination with cluster cations or macrocations has resulted in the formation of various intercluster compounds that are interesting from the viewpoints of conducting research on ionic crystals, crystal engineering, structure, sorption properties and so on. In many compounds, POMs have been combined with the independently prepared metal cluster cations [7,8].

Recently, we unexpectedly found the clusterization of monomeric phosphanegold(I) units $[\text{Au}(\text{PR}_3)]^+$ during the course of carboxylate elimination of a monomeric phosphanegold(I) carboxylate $[\text{Au}(\text{RS-pyrrld})(\text{PPh}_3)]$ ($\text{RS-Hpyrrld} = \text{RS-2-pyrrolidone-5-carboxylic acid}$). The previous representation of H_2pyrrld was changed to Hpyrrld ; thus, the formulation of $[\text{Au}(\text{RS-Hpyrrld})(\text{PPh}_3)]$ used so far was also changed to $[\text{Au}(\text{RS-pyrrld})(\text{PPh}_3)]$ [9] in the presence of the free-acid form of the Keggin POM $\text{H}_3[\alpha\text{-PW}_{12}\text{O}_{40}] \cdot 7\text{H}_2\text{O}$ [10]. This reaction resulted in the formation of a tetrakis{triphenylphosphanegold(I)} oxonium cation $[\{\{\text{Au}(\text{PPh}_3)\}_4(\mu_4\text{-O})\}]^{2+}$ as a counterion of the POM. In addition, we also found that the reaction of $[\text{Au}(\text{RS-pyrrld})(\text{PPh}_3)]$ with the sodium salt of the Keggin POM $\text{Na}_3[\alpha\text{-PW}_{12}\text{O}_{40}] \cdot 9\text{H}_2\text{O}$ gave a heptakis{triphenylphosphanegold(I)} dioxonium cation $[\{\{\text{Au}(\text{PPh}_3)\}_4(\mu_4\text{-O})\}\{\{\text{Au}(\text{PPh}_3)\}_3(\mu_3\text{-O})\}]^{3+}$ as a counterion of the POM [11]. Also, the novel intercluster compounds $[\{\{\text{Au}\{\text{P}(p\text{-RPh})_3\}\}_2(\mu\text{-OH})\}_2]_3[\alpha\text{-PM}_{12}\text{O}_{40}]_2 \cdot n\text{EtOH}$ ($R = \text{Me}, M = \text{W}; R = \text{Me}, M = \text{Mo}; R = \text{F}, M = \text{Mo}$) have been recently synthesized using the POM-mediated clusterization of monomeric para-substituted triarylphosphanegold(I) carboxylate $[\text{Au}(\text{RS-pyrrld})\{\text{P}(p\text{-RPh})_3\}]$ ($R = \text{Me}, \text{F}$) [12]. The formation of such phosphanegold(I) cluster cations was strongly dependent upon the bulkiness, acidity and charge density of the POMs, and substituents on the aryl group of phosphane ligands. The POMs appeared to act as a template in the clusterization of monomeric phosphanegold(I) units generated from the elimination of the carboxylate ligands [13,14].

The field of element-centered gold clusters $[\text{E}(\text{AuL})_n]^{m+}$ ($\text{E} =$ group 13–17 elements) has been extensively studied by the groups of Schmidbaur [15,16] and Laguna [17]. The trigold(I) oxonium cluster cations $[\{\{\text{Au}(\text{PR}_3)\}_3(\mu_3\text{-O})\}]^+$ have been reported to exhibit different forms of structural dimerization depending upon the bulkiness of phosphane ligands, *i.e.*, trigold(I) units are aggregated through crossed edges ($R = \text{Me}$) or parallel edges ($R = \text{Ph}$, *etc.*), resulting in the hexagold(I) dioxonium cluster cation as a dimer-of-trinuclear clusters $[\{\{\text{Au}(\text{PR}_3)\}_3(\mu_3\text{-O})\}_2]^{2+}$ [18–21]. Dimerization of the gold(I) cluster cations also indicates that the aurophilic interaction is the driving force for the oligomerization of many phosphanegold(I) cluster cations in the solid state. In our reported dimer-of-dinuclear gold(I) cluster cations $[\{\{\text{Au}\{\text{P}(p\text{-RPh})_3\}\}_2(\mu\text{-OH})\}_2]^{2+}$, the two digold(I) units $\{\{\text{Au}\{\text{P}(p\text{-RPh})_3\}\}_2(\mu\text{-OH})\}^+$ were dimerized by inter-cationic aurophilic interactions [12]. Also, the heptagold(I) dioxonium cluster cation $[\{\{\text{Au}(\text{PPh}_3)\}_4(\mu_4\text{-O})\}\{\{\text{Au}(\text{PPh}_3)\}_3(\mu_3\text{-O})\}]^{3+}$ was regarded as an assembly of the tetragold(I)

unit $\{\{\text{Au}(\text{PPh}_3)_4(\mu_4\text{-O})\}^{2+}$ and the trigold(I) unit $\{\{\text{Au}(\text{PPh}_3)_3(\mu_3\text{-O})\}^+$ induced by inter-cationic aurophilic interactions [11].

As continued work, we examined the POM-mediated clusterization of monomeric phosphanegold(I) units using the Keggin tungsto- and molybdo-POMs with heteroatoms P and Si, and the gold(I) carboxylate precursors with the *X*-substituted triarylphosphane ligands (*X* = *m*-F, *m*-Me and *p*-Me), $[\text{Au}(\text{RS-pyrrld})\{\text{P}(\text{XPh})_3\}]$.

In this paper, we report the syntheses and characterization of several novel intercluster compounds, $[(\text{Au}\{\text{P}(\text{m-FPh})_3\})_4(\mu_4\text{-O})]_2[\{(\text{Au}\{\text{P}(\text{m-FPh})_3\})_2(\mu\text{-OH})\}_2][\alpha\text{-PMo}_{12}\text{O}_{40}]_2 \cdot \text{EtOH}$ (**1**), $[(\text{Au}\{\text{P}(\text{m-FPh})_3\})_4(\mu_4\text{-O})]_2[\alpha\text{-SiMo}_{12}\text{O}_{40}] \cdot 4\text{H}_2\text{O}$ (**2**), $[(\text{Au}\{\text{P}(\text{m-MePh})_3\})_4(\mu_4\text{-O})]_2[\alpha\text{-SiW}_{12}\text{O}_{40}]$ (**3**), $[(\text{Au}\{\text{P}(\text{m-MePh})_3\})_4(\mu_4\text{-O})]_2[\alpha\text{-SiMo}_{12}\text{O}_{40}]$ (**4**) and $[\{(\text{Au}\{\text{P}(\text{p-MePh})_3\})_4(\mu_4\text{-O})\}\{(\text{Au}\{\text{P}(\text{p-MePh})_3\})_3(\mu_3\text{-O})\}][\alpha\text{-PW}_{12}\text{O}_{40}]$ (**5**). These compounds were formed by reactions of the Keggin POMs having varied charge densities and different acidities with the phosphanegold(I) complexes containing varied substituents on the aryl group.

2. Results and Discussion

2.1. Synthesis and Compositional Characterization

The intercluster compounds between the phosphanegold(I) cluster cations and the Keggin POM anions were obtained as **1** in 35.9% (0.089 g scale) yield, as **2** in 4.64% (0.014 g scale) yield, as **3** in 71.4% (0.247 g scale) yield, as **4** in 46.7% (0.137 g scale) yield and as **5** in 26.0% (0.026 g scale) yield. These compounds were prepared by reactions between $[\text{Au}(\text{RS-pyrrld})(\text{PR}_3)]$ (*R* = *m*-FPh (**1**, **2**), *m*-MePh (**3**, **4**) and *p*-MePh (**5**)) in CH_2Cl_2 and the Keggin POMs in mixed EtOH–H₂O solvents, *i.e.*, $\text{H}_3[\alpha\text{-PMo}_{12}\text{O}_{40}] \cdot 14\text{H}_2\text{O}$ (**1**), $\text{H}_4[\alpha\text{-SiMo}_{12}\text{O}_{40}] \cdot 12\text{H}_2\text{O}$ (**2**, **4**), $\text{H}_4[\alpha\text{-SiW}_{12}\text{O}_{40}] \cdot 10\text{H}_2\text{O}$ (**3**) and $\text{Na}_3[\alpha\text{-PW}_{12}\text{O}_{40}] \cdot 9\text{H}_2\text{O}$ (**5**). Their crystallizations were carried out by slow evaporation or liquid-liquid diffusion at room temperature. Characterization was performed by X-ray crystallography, CHN elemental analysis, thermogravimetric and differential thermal analysis (TG/DTA), Fourier transform infrared (FT-IR), solid-state cross-polarization magic-angle-spinning (CPMAS) ³¹P nuclear magnetic resonance (NMR) spectroscopy and solution (¹H, ³¹P{¹H}) NMR spectroscopy. The presence of any solvated molecules was confirmed by CHN elemental analysis, TG/DTA measurements under atmospheric conditions (Figures S1–S5), and ¹H NMR for solvated ethanol molecules.

All gold(I) cluster cations in these intercluster compounds **1–5** contained bridged-oxygen atoms such as $\mu_4\text{-O}$, $\mu_3\text{-O}$ and $\mu\text{-OH}$ groups, which were originated from water contained in the reaction system and/or the hydrated water molecules of the POMs.

The solid-state FT-IR spectra of **1–5** showed the characteristic vibrational bands on the basis of coordinating PR₃ ligands (Figures S6–S10). The FT-IR spectra also showed prominent vibrational bands owing to the α -Keggin molybdo- and tungsto-POMs [22]. In these spectra, the carbonyl vibrational bands of the anionic *RS*-pyrrld ligand in the $[\text{Au}(\text{RS-pyrrld})(\text{PR}_3)]$ precursors disappeared, showing that the carboxylate ligand was eliminated. Elimination of the carboxylate ligand was also confirmed by ¹H NMR in DMSO-*d*₆. The carboxylate plays a role of only the leaving group. In fact, not only pyrrolidone carboxylate, but also other carboxylates such as 5-oxotetrahydrofuran-2-carboxylate and acetylglycinate can serve as the leaving groups in the formation of the tetragold(I) clusters in the presence of POMs [10].

Table 1. Crystallographic data for 1–5.

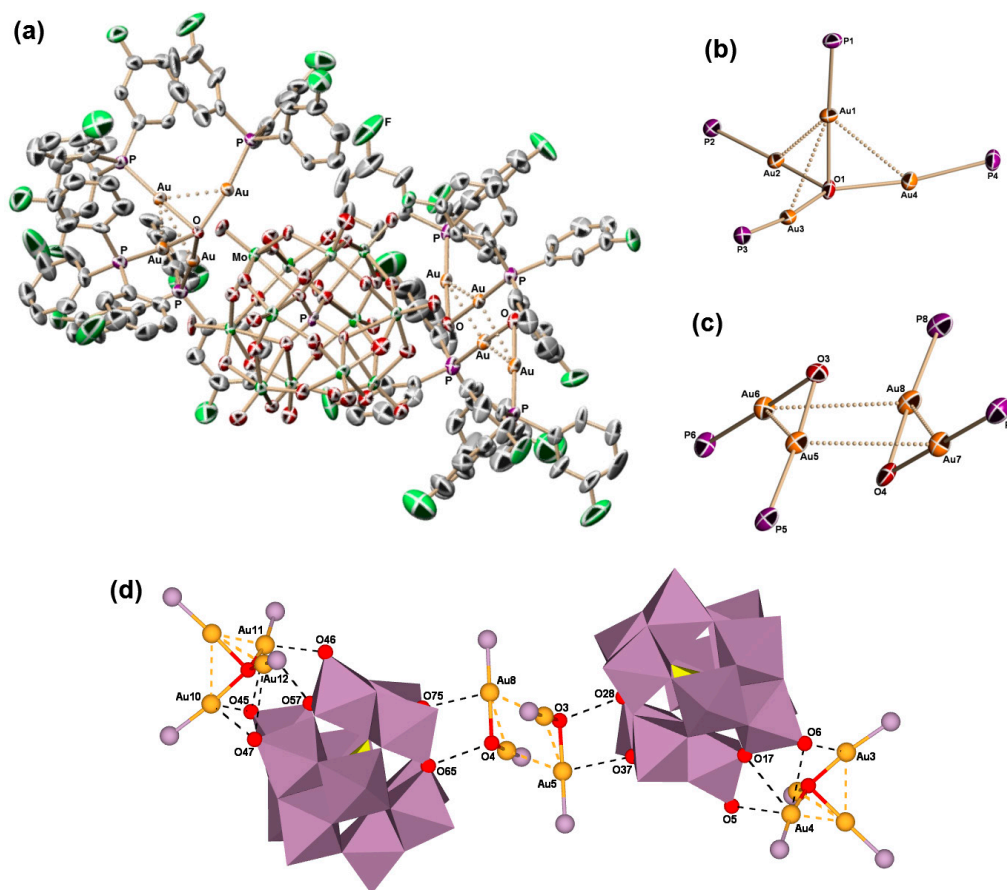
Parameters	1	2	3	4	5
Formula	C ₂₁₆ H ₁₄₆ Au ₁₂ F ₃₆ -Mo ₂₄ O ₈₄ P ₁₄	C ₁₄₄ H ₁₀₄ Au ₈ F ₂₄ -Mo ₁₂ O ₄₆ P ₈ Si	C ₁₆₈ H ₁₆₈ Au ₈ O ₄₆ -P ₈ SiW ₁₂	C ₁₆₈ H ₁₆₈ Au ₈ Mo ₁₂ -O ₄₆ P ₈ Si	C ₁₄₇ H ₁₄₇ Au ₇ O ₄₂ -P ₈ W ₁₂
Formula weight	9869.07	6029.13	6980.81	5925.89	6418.37
Color, shape	Orange-yellow, rod	Yellow, block	Pale-yellow, block	Yellow, block	Colorless, plate
Crystal system	Triclinic	Triclinic	Rhombohedral	Rhombohedral	Triclinic
Space group	<i>P</i> -1	<i>P</i> -1	<i>R</i> -3	<i>R</i> -3	<i>P</i> -1
<i>T</i> /K	100	120	120	100	100
<i>a</i> /Å	16.191(2)	16.296(3)	20.478(3)	20.3813(7)	17.7243(11)
<i>b</i> /Å	29.165(4)	16.357(3)			17.8341(10)
<i>c</i> /Å	35.365(4)	16.854(3)	36.726(7)	36.679(2)	31.7570(18)
α /°	99.801(2)	77.37(3)			104.8260(10)
β /°	99.153(2)	75.89(3)			92.640(2)
γ /°	104.963(2)	80.58(3)	120	120	109.6850(10)
<i>V</i> /Å ³	15533(3)	4222.3(15)	13337(4)	13195.2(11)	9040.0(9)
<i>Z</i>	2	1	3	3	2
<i>D</i> _{calc} /g cm ⁻³	2.110	2.371	2.607	2.237	2.358
<i>F</i> ₀₀₀	9208	2822	9594	8442	5852
GOF	1.027	1.066	1.311	1.074	1.373
<i>R</i> ₁ (<i>I</i> > 2.00 σ (<i>I</i>))	0.0723	0.0915	0.0547	0.0376	0.1466
<i>R</i> (all data)	0.1077	0.1042	0.0558	0.0390	0.2417
w <i>R</i> ₂ (all data)	0.1753	0.2502	0.1217	0.0862	0.4614

2.2. Molecular Structures of 1–5

Crystal data of **1–5** were given in Table 1. Bond lengths (Å) and angles (°) for **1–5** were shown in Supplementary Information (Tables S1–S5).

Single-crystal X-ray analysis revealed that **1** crystallizes in the Triclinic *P*-1 space group, and is composed of two tetragold(I) cluster cations $[(\text{Au}\{\text{P}(m\text{-FPh})_3\})_4(\mu_4\text{-O})]^{2+}$ and one dimer-of-dinuclear gold(I) cluster cation $[\{(\text{Au}\{\text{P}(m\text{-FPh})_3\})_2(\mu\text{-OH})\}_2]^{2+}$, and two Keggin POM anions $[\alpha\text{-PMo}_{12}\text{O}_{40}]^{3-}$ as counterions (Figure 1a).

Figure 1. (a) Molecular structure of **1**; (b) The partial structure of the tetragold(I) cluster cation moiety; (c) The partial structure of the dimer-of-dinuclear gold(I) cluster cation moiety; (d) The interactions among the tetragold(I) cluster cations, dimer-of-dinuclear gold(I) cluster cation and Keggin polyoxometalate (POM) anions.



The two tetragold(I) cluster cations $[(\text{Au}\{\text{P}(m\text{-FPh})_3\})_4(\mu_4\text{-O})]^{2+}$ adopt trigonal-pyramidal structures composed of three short edges associated with (Au1, Au2, Au3, Au4) atoms and (Au9, Au10, Au11, Au12) atoms, respectively (Au1–Au2: 2.9513 Å, Au1–Au3: 2.8978 Å, Au1–Au4: 2.8582 Å; Au9–Au10: 2.9293 Å, Au9–Au11: 2.8719 Å, Au9–Au12: 3.0815 Å), and a triangular plane of (Au2, Au3, Au4) atoms and (Au10, Au11, Au12) atoms, respectively, with longer edge lengths (Au2–Au3: 3.650 Å, Au2–Au4: 3.655 Å, Au3–Au4: 3.536 Å; Au10–Au11: 3.568 Å, Au10–Au12: 3.528 Å, Au11–Au12: 3.717 Å) (Figure 1b). The bridged-oxygen atoms ($\mu_4\text{-O}$) were placed within the basal plane composed of (Au2, Au3, Au4) atoms and (Au10, Au11, Au12) atoms, respectively (Au2–O1–Au3: 123.6°,

Au2–O1–Au4: 120.0°, Au3–O1–Au4: 116.1°; Au10–O2–Au11: 117.4°, Au10–O2–Au12: 116.2°, Au11–O2–Au12: 126.4°), resulting in a point group of C_{3v} for the tetragold(I) cluster cations. The distorted tetragold(I) cluster cations in **1** are similar to that of the previously reported tetragold(I) cluster cation $[(\text{Au}(\text{PPh}_3))_4(\mu_4\text{-O})]^{2+}$ as the counterion of the POM [10,13].

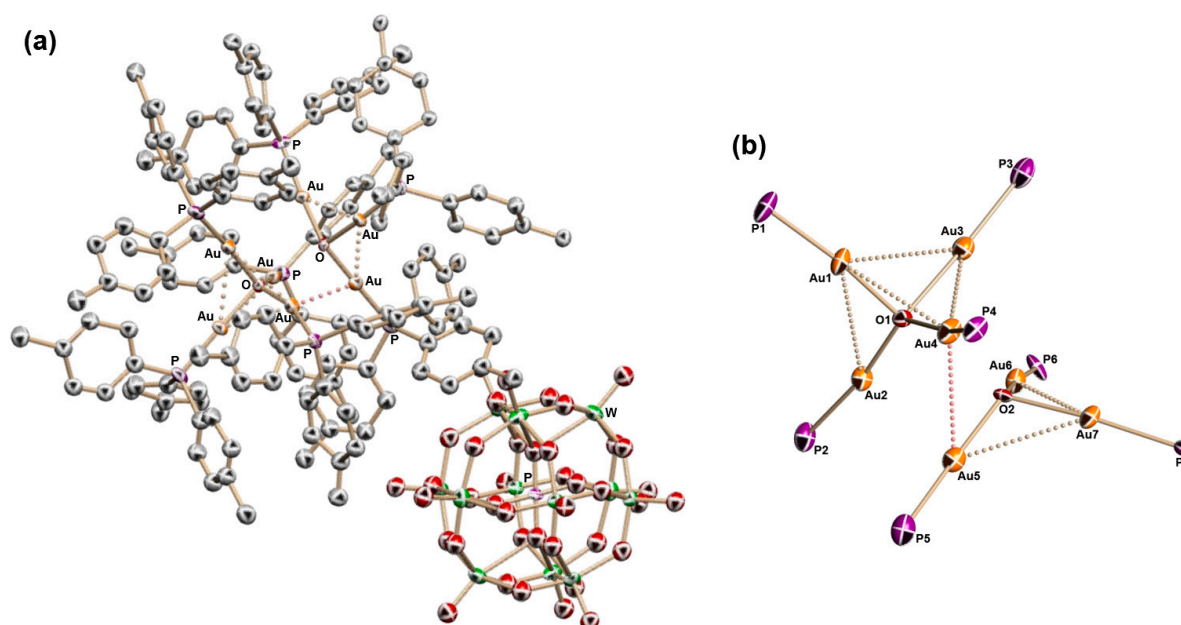
The dimer-of-dinuclear gold(I) cluster cation in **1** can be regarded as the dimerization of digold(I) units $\{(\text{Au}\{\text{P}(m\text{-FPh})_3\})_2(\mu\text{-OH})\}^+$. The digold(I) unit consists of two monomer subunits $(\text{Au}\{\text{P}(m\text{-FPh})_3\})^+$ linked by a $\mu\text{-OH}$ group and is triangular in shape. Two digold(I) units dimerize to form the dimer-of-dinuclear gold(I) cluster cation $[(\text{Au}\{\text{P}(m\text{-FPh})_3\})_2(\mu\text{-OH})]_2^{2+}$ in a parallel-edge arrangement by inter-cationic aurophilic interactions (Au5–Au7: 3.2921 Å, Au6–Au8: 3.3454 Å) (Figure 1c). The dimer-of-dinuclear gold(I) cluster cation of a parallel-edge arrangement in **1** is similar to that of the previously reported dimer-of-dinuclear gold(I) cluster cation $[(\text{Au}\{\text{P}(p\text{-FPh})_3\})_2(\mu\text{-OH})]_2^{2+}$ with $[\alpha\text{-PMo}_{12}\text{O}_{40}]^{3-}$ [12].

The five gold(I) atoms Au3, Au4, Au10, Au11 and Au12 in the tetragold(I) cluster cation moiety interact with the terminal oxygen atoms and OMo2 oxygen atoms of edge-shared MoO₆ octahedra of the Keggin POMs (Au3–O6: 2.943 Å, Au4–O5: 3.143 Å, Au4–O6: 3.136 Å, Au4–O17: 3.087 Å, Au10–O45: 3.179 Å, Au10–O47: 3.143 Å, Au11–O45: 3.112 Å, Au11–O46: 3.023 Å, Au11–O57: 3.047 Å, Au12–O47: 3.123 Å). The two gold(I) atoms Au5 and Au8 in the dimer-of-dinuclear gold(I) cluster cation moiety interact with the OMo2 oxygen atoms of edge-shared MoO₆ octahedra of the Keggin POMs (Au5–O37: 2.945 Å, Au8–O75: 2.853 Å), and the short distances between dimer-of-dinuclear gold(I) cluster cation and Keggin POMs indicate the existence of a hydrogen bonding (O3–O28: 3.021 Å, O4–O65: 3.043 Å) (Figure 1d). The meta-substituted triarylphosphane ligand was few influence for the POM-mediated clusterization of monomeric phosphanegold(I) units.

Single-crystal X-ray analysis revealed that **2** crystallizes in the Triclinic $P\bar{1}$ space group, and is composed of two tetragold(I) cluster cations $[(\text{Au}\{\text{P}(m\text{-FPh})_3\})_4(\mu_4\text{-O})]^{2+}$ and one Keggin POM anion $[\alpha\text{-SiMo}_{12}\text{O}_{40}]^{4-}$ as counterion (Figure S11a). Single-crystal X-ray analysis also revealed that **3** and **4** crystallize in the Rhombohedral $R\bar{3}$ space group, respectively, and are composed of two tetragold(I) cluster cations, $[(\text{Au}\{\text{P}(m\text{-MePh})_3\})_4(\mu_4\text{-O})]^{2+}$, and one Keggin POM anion $[\alpha\text{-SiW}_{12}\text{O}_{40}]^{4-}$ for **3** (Figure S12) and $[\alpha\text{-SiMo}_{12}\text{O}_{40}]^{4-}$ for **4** as counterions.

The tetragold(I) cluster cation $[(\text{Au}\{\text{P}(m\text{-FPh})_3\})_4(\mu_4\text{-O})]^{2+}$ of **2** was very similar to that of **1** (C_{3v} symmetry) (Figure S11b). The three gold(I) atoms Au2, Au3 and Au4 in the tetragold(I) cluster cation interact with the OMo2 oxygen atoms of edge-shared MoO₆ octahedra and terminal oxygen atoms of the Keggin POM (Au2–O4: 3.094 Å, Au2–O9: 3.070 Å, Au3–O3: 3.139 Å, Au3–O8: 3.021 Å, Au4–O10: 2.916 Å). The tetragold(I) cluster cations $[(\text{Au}\{\text{P}(m\text{-MePh})_3\})_4(\mu_4\text{-O})]^{2+}$ of **3** and **4** adopt trigonal-pyramidal structures (C_{3v} symmetry) due to interactions with the Keggin POMs (Au2–O3: 3.178 Å, Au2–O7: 2.994 Å for **3**; Au2–O2: 3.144 Å, Au2–O4: 2.929 Å for **4**). The Keggin POM anion was disordered. Compound **4** is isostructural with **3**, with the different metal atom (W vs. Mo) in the Keggin POM anion.

Single-crystal X-ray analysis revealed that **5** crystallizes in the Triclinic $P\bar{1}$ space group, and is composed of a heptagold(I) cluster cation $[(\text{Au}\{\text{P}(p\text{-MePh})_3\})_4(\mu_4\text{-O})\{(\text{Au}\{\text{P}(p\text{-MePh})_3\})_3(\mu_3\text{-O})\}]^{3+}$ and one Keggin POM anion $[\alpha\text{-PW}_{12}\text{O}_{40}]^{3-}$ as counterion (Figure 2a). However, the crystals of **5** were not suitable for X-ray analysis. Although the existence of the heptagold(I) cluster cation was confirmed, the quality of the crystal data was poor (Table 1).

Figure 2. (a) Molecular structure of **5**; (b) The partial structure of the heptagold(I) cluster cation.

The heptagold(I) cluster cation was composed of the tetragold(I) cluster cation and trigold(I) cluster cation (Figure 2b). Two gold(I) cluster cations were linked by the one inter-cationic aurophilic interaction (Au4–Au5: 3.034 Å). The aurophilic interaction is longer than the Au–Au separation of metallic gold (2.88 Å) [23], but shorter than twice the van der Waals radius for gold (3.32 Å) [24]. In comparison with the previously reported heptagold(I) cluster cation [$\{\{\text{Au}(\text{PPh}_3)\}_4(\mu_4\text{-O})\}\{\{\text{Au}(\text{PPh}_3)\}_3(\mu_3\text{-O})\}\}^{3+}$] [11], the heptagold(I) cluster cation in **5** has a similar structure, but the number of inter-cationic aurophilic interaction was decreased. This different coupled structure is produced by steric effects of the methyl groups in the para-substituted triarylphosphane ligands. On the other hand, the bridged-oxygen–oxygen distance (O1–O2: 2.830 Å) in the heptagold(I) cluster cation in **5** is shorter than that (3.096 Å) of the previously reported heptagold(I) cluster cation. This oxygen–oxygen distance is also shorter than twice the van der Waals radius for oxygen (3.04 Å) [24]. The tetragold(I) cluster moiety had a distorted tetrahedron structure due to four intra-cationic aurophilic interactions (Au1–Au2: 3.308 Å, Au1–Au3: 3.112 Å, Au1–Au4: 3.064 Å, Au3–Au4: 3.111 Å). The encapsulated oxygen atom ($\mu_4\text{-O}$) was placed within the distorted tetrahedron (Au2–O1–Au3: 126.9°, Au2–O1–Au4: 129.4°, Au3–O1–Au4: 92.4°; total 348.7°). The trigold(I) cluster moiety composed of two intra-cationic aurophilic interactions (Au5–Au7: 3.199 Å, Au6–Au7: 3.078 Å) and one long Au–Au edge (Au5–Au6: 3.606 Å) formed a triangular plane of the (Au5, Au6, Au7) atoms. The bridged-oxygen atom ($\mu_3\text{-O}$) was placed out-of-plane consisting a triangular plane of the three gold(I) atoms (Au5–O2–Au6: 127.9°, Au5–O2–Au7: 104.0°, Au6–O2–Au7: 98.2°; total 330.1°). Probably, the heptagold(I) cluster cation would be formed by the clusterization of monomeric triarylphosphanegold(I) units $[\text{Au}(\text{PR}_3)]^+$ with smaller steric effects in the presence of the less-acidic POM, *i.e.*, $\text{Na}_3[\alpha\text{-PW}_{12}\text{O}_{40}] \cdot 9\text{H}_2\text{O}$ [11].

2.3. Solid-State CPMAS ^{31}P and Solution $^{31}\text{P}\{^1\text{H}\}$ NMR

The solid-state CPMAS ^{31}P and solution $^{31}\text{P}\{^1\text{H}\}$ NMR in DMSO- d_6 signals of **1–5** are listed in Table 2. The solid-state CPMAS ^{31}P NMR of **1** observed two broad signals at –3.4 and 24.4 ppm.

The signal at -3.4 ppm is assignable to the heteroatom phosphorus in the Keggin molybdo-POM anion, and the signal at 24.4 ppm is assignable to the overlapped signals of the tetragold(I) cluster cations and the dimer-of-dinuclear gold(I) cluster cation. The solid-state CPMAS ^{31}P NMR of **2**, **3** and **4** showed two broad signals at 19.6 and 24.4 ppm for **2**, 18.3 and 28.5 ppm for **3**, 17.4 and 27.7 ppm for **4** originating from the inequivalent phosphane groups. The three signals at 19.6 , 18.3 and 17.4 ppm are assignable to one apical phosphane group, respectively, and the other three signals at 24.4 , 28.5 and 27.7 ppm are assignable to the three basal phosphane groups in the trigonal-pyramidal structure, respectively [10,13]. The solid-state CPMAS ^{31}P NMR of **5** showed two broad signals at -14.6 and 23.1 ppm due to the Keggin tungsto-POM anion and phosphane groups of the heptagold(I) cluster cation, respectively. Although all phosphane groups of the heptagold(I) cluster cation are inequivalent as shown in X-ray analysis, their signals were observed as one broad peak at 23.1 ppm.

Table 2. Solid-state cross-polarization magic-angle-spinning (CPMAS) ^{31}P and solution $^{31}\text{P}\{^1\text{H}\}$ nuclear magnetic resonance (NMR) in DMSO- d_6 signals (ppm) of **1–5**.

Compound	Solid-State CPMAS ^{31}P	Solution $^{31}\text{P}\{^1\text{H}\}$
1	$-3.4, 24.4$	$-3.23, 26.31$ (main), $-0.40, 43.57$ (minor)
2	$19.6, 24.4$	25.67 (main), 43.38 (minor)
3	$18.3, 28.5$	insoluble
4	$17.4, 27.7$	insoluble
5	$-14.6, 23.1$	$-14.88, 22.39$

The solution $^{31}\text{P}\{^1\text{H}\}$ NMR signals of **1**, **2** and **5** in DMSO- d_6 were observed as major sharp signals at 26.31 , 25.67 and 22.39 ppm, respectively. These signals were shifted to a higher field from the monomeric phosphanegold(I) precursors (29.20 and 25.35 ppm), respectively. In general, the $^{31}\text{P}\{^1\text{H}\}$ NMR signals of oxygen-centered phosphanegold(I) clusters are observed in the higher field in comparison with those of the monomeric phosphanegold(I) precursors [10–12]. The peak at -3.23 ppm for **1** and -14.88 ppm for **5** are assignable to the heteroatom phosphorus in the Keggin POMs ($M = \text{Mo}, \text{W}$). Because Keggin molybdo-POMs are unstable in DMSO, the minor signals at -0.40 , 43.57 ppm of **1** and 43.38 ppm of **2** are assignable to the decomposition species. Because **3** and **4** are insoluble in any solvents, the solution $^{31}\text{P}\{^1\text{H}\}$ NMR data of **3** and **4** were not obtained.

3. Experimental Section

3.1. Materials

The following reactants were used as received: EtOH, CH_2Cl_2 , Et₂O (all from Wako, Osaka, Japan), and DMSO- d_6 (Isotec, Miamisburg, OH, USA). With respect to the α -Keggin POMs, $\text{H}_3[\alpha\text{-PMo}_{12}\text{O}_{40}] \cdot 14\text{H}_2\text{O}$, $\text{H}_4[\alpha\text{-SiMo}_{12}\text{O}_{40}] \cdot 12\text{H}_2\text{O}$, $\text{H}_4[\alpha\text{-SiW}_{12}\text{O}_{40}] \cdot 10\text{H}_2\text{O}$ and $\text{Na}_3[\alpha\text{-PW}_{12}\text{O}_{40}] \cdot 9\text{H}_2\text{O}$ were prepared according to the ether extraction method [25] and the literatures [26,27], and identified by FT-IR, TG/DTA and solution (^{29}Si , ^{31}P , ^{183}W) NMR spectroscopy. The $[\text{Au}(\text{RS-pyrrld})\{\text{P}(m\text{-XPh})_3\}]$ ($X = \text{F}, \text{Me}$) and $[\text{Au}(\text{RS-pyrrld})\{\text{P}(p\text{-MePh})_3\}]$ precursor complexes were synthesized according to the reported methods using $\text{P}(m\text{-XPh})_3$ ($X = \text{F}, \text{Me}$) or $\text{P}(p\text{-MePh})_3$ [9,12], and characterized by CHN elemental analysis, FT-IR, TG/DTA and solution (^1H , $^{13}\text{C}\{^1\text{H}\}$, $^{31}\text{P}\{^1\text{H}\}$) NMR spectroscopy.

3.2. Instrumentation and Analytical Procedures

CHN elemental analyses were carried out with a Perkin-Elmer (Waltham, MA, USA) 2400 CHNS Elemental Analyzer II (Kanagawa University, Kanagawa, Japan). IR spectra were recorded on a Jasco (Tokyo, Japan) 4100 FT-IR spectrometer in KBr disks at room temperature. TG/DTA were acquired using a Rigaku (Tokyo, Japan) Thermo Plus 2 series TG 8120 instrument. ^1H NMR (500.00 MHz) and $^{31}\text{P}\{^1\text{H}\}$ NMR (202.00 MHz) spectra in a DMSO- d_6 solution were recorded in 5-mm-outer-diameter tubes on a JEOL (Tokyo, Japan) JNM-ECP 500 FT-NMR spectrometer with a JEOL (Tokyo, Japan) ECP-500 NMR data processing system. The ^1H NMR spectra were referenced to an internal standard of tetramethylsilane (SiMe_4). The $^{31}\text{P}\{^1\text{H}\}$ NMR spectra were referenced to an external standard of 25% H_3PO_4 in H_2O in a sealed capillary. The $^{31}\text{P}\{^1\text{H}\}$ NMR data with the usual 85% H_3PO_4 reference are shifted to +0.544 ppm from our data. Solid-state CPMAS ^{31}P NMR (121.00 MHz) spectra were recorded in 6-mm-outer-diameter rotors on a JEOL JNM-ECP 300 FT-NMR spectrometer with a JEOL ECP-300 NMR data processing system. The spectra were referenced to an external standard of $(\text{NH}_4)_2\text{HPO}_4$ (δ 1.60).

3.3. Syntheses

$[(\text{Au}\{\text{P}(m\text{-FPh})_3\})_4(\mu_4\text{-O})]_2\{(\text{Au}\{\text{P}(m\text{-FPh})_3\})_2(\mu\text{-OH})\}_2][\alpha\text{-PMo}_{12}\text{O}_{40}]_2\cdot\text{EtOH}$ (**1**): A solution of $[\text{Au}(\text{RS-pyrrld})\{\text{P}(m\text{-FPh})_3\}]$ (0.192 g, 0.300 mmol) dissolved in 25 mL of CH_2Cl_2 was slowly added to a yellow clear solution of $\text{H}_3[\alpha\text{-PMo}_{12}\text{O}_{40}]\cdot 14\text{H}_2\text{O}$ (0.104 g, 0.050 mmol) dissolved in 15 mL of an $\text{EtOH}\text{-H}_2\text{O}$ (5:1, v/v) mixed solvent. After stirring for 1 h at room temperature, the reaction solution was filtered through a folded filter paper (Whatman, Maidstone, UK, No. 5). The resulting yellow clear solution was slowly evaporated at room temperature in the dark. After 7 days, the orange yellow rod crystals were formed, and collected on a membrane filter (JG 0.2 μm), washed with EtOH (20 mL \times 2) and Et_2O (20 mL \times 2), and dried *in vacuo* for 2 h. Yield: 0.089 g (35.9%). The crystalline samples were soluble in DMSO, but insoluble in H_2O , EtOH and Et_2O . Calcd. for $\text{C}_{218}\text{H}_{152}\text{O}_{85}\text{F}_{36}\text{P}_{14}\text{Mo}_{24}\text{Au}_{12}$ or $[(\text{Au}\{\text{P}(m\text{-FPh})_3\})_4(\mu_4\text{-O})]_2\{(\text{Au}\{\text{P}(m\text{-FPh})_3\})_2(\mu\text{-OH})\}_2][\alpha\text{-PMo}_{12}\text{O}_{40}]_2\cdot\text{EtOH}$: C, 26.41; H, 1.55%. Found: C, 26.35; H, 1.15%. TG/DTA under atmospheric conditions: a weight loss of 1.22% because of desorption of EtOH was observed at temperature less than 200.5 $^\circ\text{C}$; calcd. 1.38% for three EtOH molecules. IR (KBr) (cm^{-1}): 1601 w, 1581 s, 1522 vw, 1476 m, 1422 m, 1305 vw, 1268 w, 1225 s, 1165 vw, 1096 w, 1062 m, 1000 vw, 957 s, 876 m, 812 vs, 782 vs, 682 m, 614 vw, 583 w, 522 w, 510 w, 481 w, 470 w, 409 w. $^{31}\text{P}\{^1\text{H}\}$ NMR (25.5 $^\circ\text{C}$, DMSO- d_6): δ -3.23, 26.31 (main), -0.40, 43.57 (minor) ppm. ^1H NMR (24.7 $^\circ\text{C}$, DMSO- d_6): δ 1.09 (t, J = 7.1 Hz, $\text{CH}_3\text{CH}_2\text{OH}$ solvate), 3.38 (q, J = 7.0 Hz, $\text{CH}_3\text{CH}_2\text{OH}$ solvate), 7.35–7.57 (m, *Aryl*) ppm. Solid-state CPMAS ^{31}P NMR (R.T.): δ -3.4, 24.4 ppm.

$[(\text{Au}\{\text{P}(m\text{-FPh})_3\})_4(\mu_4\text{-O})]_2[\alpha\text{-SiMo}_{12}\text{O}_{40}]\cdot 4\text{H}_2\text{O}$ (**2**): In the synthesis of **1**, $\text{H}_4[\alpha\text{-SiMo}_{12}\text{O}_{40}]\cdot 12\text{H}_2\text{O}$ (0.102 g, 0.050 mmol) was used instead of $\text{H}_3[\alpha\text{-PMo}_{12}\text{O}_{40}]\cdot 14\text{H}_2\text{O}$, and $[\text{Au}(\text{RS-pyrrld})\{\text{P}(m\text{-FPh})_3\}]$ (0.257 g, 0.400 mmol) was also used. After 10 days, the yellow block crystals were formed. Yield: 0.014 g (4.64%). The crystalline samples were soluble in DMSO, but insoluble in H_2O , EtOH and Et_2O . Calcd. for $\text{C}_{144}\text{H}_{104}\text{O}_{46}\text{F}_{24}\text{Si}_1\text{P}_8\text{Mo}_{12}\text{Au}_8$ or $[(\text{Au}\{\text{P}(m\text{-FPh})_3\})_4(\mu_4\text{-O})]_2[\alpha\text{-SiMo}_{12}\text{O}_{40}]\cdot 4\text{H}_2\text{O}$: C, 28.69; H, 1.74%. Found: C, 29.10; H, 1.49%. TG/DTA under atmospheric conditions: a weight loss of 1.07% because of desorption of H_2O was observed at temperature less than 240.4 $^\circ\text{C}$; calcd. 1.19% for four H_2O molecules.

IR (KBr) (cm^{-1}): 1601 m, 1579 s, 1475 m, 1420 m, 1305 vw, 1268 w, 1225 s, 1163 vw, 1095 w, 999 vw, 984 vw, 943 m, 900 vs, 870 m, 806 vs, 796 vs, 784 vs, 691 s, 683 s, 628 m, 583 s, 523 s, 511 s, 469 s. $^{31}\text{P}\{^1\text{H}\}$ NMR (26.4 °C, DMSO-*d*₆): δ 25.67 (main), 43.38 (minor) ppm. ^1H NMR (25.0 °C, DMSO-*d*₆): δ 7.37–7.72 (m, *Aryl*) ppm. Solid-state CPMAS ^{31}P NMR (R.T.): δ 19.6, 24.4 ppm.

$[(\text{Au}\{\text{P}(m\text{-MePh})_3\})_4(\mu_4\text{-O})]_2[\alpha\text{-SiW}_{12}\text{O}_{40}]$ (**3**): In the synthesis of **2**, $\text{H}_4[\alpha\text{-SiW}_{12}\text{O}_{40}] \cdot 10\text{H}_2\text{O}$ (0.153 g, 0.050 mmol) was used instead of $\text{H}_4[\alpha\text{-SiMo}_{12}\text{O}_{40}] \cdot 12\text{H}_2\text{O}$, and $[\text{Au}(\text{RS-pyrrld})\{\text{P}(m\text{-MePh})_3\}]$ (0.252 g, 0.400 mmol) was also used in place of $[\text{Au}(\text{RS-pyrrld})\{\text{P}(m\text{-FPh})_3\}]$. After 10 days, the pale-yellow block crystals were formed. Yield: 0.247 g (71.4%). The crystalline samples were insoluble in H_2O , EtOH, Et₂O and DMSO. Calcd. for $\text{C}_{168}\text{H}_{168}\text{O}_{42}\text{Si}_1\text{P}_8\text{W}_{12}\text{Au}_8$ or $[(\text{Au}\{\text{P}(m\text{-MePh})_3\})_4(\mu_4\text{-O})]_2[\alpha\text{-SiW}_{12}\text{O}_{40}]$: C, 29.17; H, 2.45%. Found: C, 28.68; H, 2.17%. TG/DTA under atmospheric conditions: no weight loss was observed at below 214.6 °C. IR (KBr) (cm^{-1}): 1592 w, 1576 w, 1476 m, 1448 m, 1403 m, 1379 w, 1311 w, 1277 vw, 1221 w, 1174 vw, 1108 m, 1039 vw, 1010 m, 996 w, 970 vs, 921 vs, 881 s, 805 vs, 691 vs, 569 m, 561 m, 531 s, 491 m, 465 m, 450 s. Solid-state CPMAS ^{31}P NMR (R.T.): δ 18.3, 28.5 ppm.

$[(\text{Au}\{\text{P}(m\text{-MePh})_3\})_4(\mu_4\text{-O})]_2[\alpha\text{-SiMo}_{12}\text{O}_{40}]$ (**4**): $[\text{Au}(\text{RS-pyrrld})\{\text{P}(m\text{-MePh})_3\}]$ (0.252 g, 0.400 mmol) was dissolved in 25 mL of CH_2Cl_2 . A yellow clear solution of $\text{H}_4[\alpha\text{-SiMo}_{12}\text{O}_{40}] \cdot 12\text{H}_2\text{O}$ (0.102 g, 0.050 mmol) dissolved in 15 mL of an EtOH– H_2O (5:1, v/v) mixed solvent was slowly added along an interior wall of a round-bottomed flask containing a colorless clear solution of the phosphanegold(I) complex. The round-bottomed flask containing two layers was sealed and left in the dark at room temperature. After 7 days, the yellow block crystals formed around the interface of the two layers, which were collected on a membrane filter (JG 0.2 μm), washed with EtOH (20 mL \times 2) and Et₂O (20 mL \times 2), and dried *in vacuo* for 2 h. Yield: 0.137 g (46.7%). The crystalline samples were insoluble in H_2O , EtOH, Et₂O and DMSO. Calcd. for $\text{C}_{168}\text{H}_{168}\text{O}_{42}\text{Si}_1\text{P}_8\text{Mo}_{12}\text{Au}_8$ or $[(\text{Au}\{\text{P}(m\text{-MePh})_3\})_4(\mu_4\text{-O})]_2[\alpha\text{-SiMo}_{12}\text{O}_{40}]$: C, 34.42; H, 2.89%. Found: C, 34.35; H, 2.70%. TG/DTA under atmospheric conditions: no weight loss was observed at below 222.4 °C. IR (KBr) (cm^{-1}): 1591 w, 1575 w, 1475 w, 1446 w, 1403 w, 1310 vw, 1221 vw, 1174 vw, 1107 w, 1040 vw, 995 vw, 983 w, 947 s, 902 vs, 861 m, 804 vs, 794 vs, 691 m, 681 m, 568 w, 532 w, 491 w, 465 w, 449 m. Solid-state CPMAS ^{31}P NMR (R.T.): δ 17.4, 27.7 ppm.

$\{[(\text{Au}\{\text{P}(p\text{-MePh})_3\})_4(\mu_4\text{-O})]\{(\text{Au}\{\text{P}(p\text{-MePh})_3\})_3(\mu_3\text{-O})\}][\alpha\text{-PW}_{12}\text{O}_{40}]$ (**5**): A solution of $[\text{Au}(\text{RS-pyrrld})\{\text{P}(p\text{-MePh})_3\}]$ (0.189 g, 0.300 mmol) dissolved in 25 mL of CH_2Cl_2 was slowly added to a colorless clear solution of $\text{Na}_3[\alpha\text{-PW}_{12}\text{O}_{40}] \cdot 9\text{H}_2\text{O}$ (0.155 g, 0.050 mmol) dissolved in 15 mL of an EtOH– H_2O (5:1, v/v) mixed solvent. After stirring for 1 h at room temperature, the reaction solution was concentrated to 15 mL with a rotary evaporator at 30 °C. A pale-yellow white powder was collected on a membrane filter (JV 0.1 μm), washed with H_2O (20 mL \times 2), EtOH (20 mL \times 2) and Et₂O (20 mL \times 2), and dried *in vacuo* for 2 h. At this stage, the pale-yellow white powder was obtained in a yield of 0.23 g.

Crystallization. The pale-yellow white powder (0.100 g) was dissolved in 20 mL of a CH_2Cl_2 –EtOH (3:1, v/v) mixed solvent and was filtered through a folded filter paper (Whatman No. 5). The pale-yellow clear filtrate was slowly evaporated at room temperature in the dark. After 3 days, colorless plate crystals were formed and collected on a membrane filter (JV 0.1 μm), washed with EtOH (10 mL \times 2) and Et₂O (10 mL \times 2), and dried *in vacuo* for 2 h. Yield: 0.026 g (26.0%). The crystalline samples were soluble in DMSO and sparingly soluble in CH_2Cl_2 , but insoluble in H_2O , EtOH and Et₂O. Calcd. for $\text{C}_{147}\text{H}_{147}\text{O}_{42}\text{P}_8\text{W}_{12}\text{Au}_7$ or $\{[(\text{Au}\{\text{P}(p\text{-MePh})_3\})_4(\mu_4\text{-O})]\{(\text{Au}\{\text{P}(p\text{-MePh})_3\})_3(\mu_3\text{-O})\}][\alpha\text{-PW}_{12}\text{O}_{40}]$:

C, 27.51; H, 2.31%. Found: C, 27.51; H, 2.63%. TG/DTA under atmospheric conditions: no weight loss was observed at below 203.6 °C. IR (KBr) (cm^{-1}): 1597 w, 1496 w, 1445 w, 1397 w, 1309 vw, 1189 w, 1103 m, 1079 s, 977 s, 896 m, 821 vs, 802 vs, 706 w, 647 w, 633 w, 619 w, 526 m, 510 m. $^{31}\text{P}\{^1\text{H}\}$ NMR (26.7 °C, DMSO- d_6): δ -14.88, 22.39 ppm. ^1H NMR (25.6 °C, DMSO- d_6): δ 2.25 (s, *Me*), 7.10–7.30 (m, *Aryl*) ppm. Solid-state CPMAS ^{31}P NMR (R.T.): δ -14.6, 23.1 ppm.

3.4. X-ray Crystallography

Single crystals with dimensions of $0.30 \times 0.08 \times 0.07 \text{ mm}^3$ for **1**, $0.06 \times 0.06 \times 0.04 \text{ mm}^3$ for **2**, $0.23 \times 0.13 \times 0.07 \text{ mm}^3$ for **3**, $0.31 \times 0.26 \times 0.15 \text{ mm}^3$ for **4** and $0.08 \times 0.07 \times 0.02 \text{ mm}^3$ for **5** were mounted on cryoloops using liquid paraffin and cooled by a stream of cooled N_2 gas. Data collection was performed on a Bruker (Madison, WI, USA) SMART APEX CCD diffractometer at 100 K for **1**, **4** and **5**, and Rigaku (Tokyo, Japan) VariMax with Saturn CCD diffractometer at 120 K for **2** and **3**. The intensity data were automatically collected for Lorentz and polarization effects during integration. The structure was solved by direct methods (program *SHELXS-97*) followed by subsequent difference Fourier calculation and refined by a full-matrix, least-squares procedure on F^2 (program *SHELXL-97*) [28]. Absorption correction was performed with *SADABS* (empirical absorption correction) [29]. The compositions and formulae of the POMs containing many solvated molecules were determined by CHN elemental analysis, TG/DTA and ^1H NMR. Any solvent molecules in the structure were highly disordered and impossible to refine by using conventional discrete-atom models. To resolve these issues, the contribution of the solvent electron density was removed by using the *SQUEEZE* routine in *PLATON* for **1** [30]. The details of the crystallographic data for **1–5** are listed in Table 1, and bond lengths (Å) and angles (°) for **1–5** are shown in Tables S1–S5. CCDC 1028278 (**1**), 1028279 (**2**), 1028280 (**3**), 1028281 (**4**) and 1028282 (**5**), respectively. Polyhedral representation in Figure 1 was drawn by using the VESTA 3 series [31].

4. Conclusions

In this paper, we prepared and characterized various novel intercluster compounds **1–5** by POM-mediated clusterization. Formation of these gold(I) cluster cations in **1–5** was strongly dependent upon the charge density and acidity of the POMs, and substituted position on the aryl group of triarylphosphane ligands as well. The structures of phosphanegold(I) cluster cations were stabilized by the intra-cluster and inter-cluster aurophilic interactions, and also interactions between the gold(I) cluster cations and POM anions. The two free-acid forms of Keggin POMs with heteroatom Si provided the trigonal-pyramidal structures of the tetraphosphanegold(I) cluster cations in the intercluster compounds, *i.e.*, $[(\text{Au}\{\text{P}(m\text{-FPh})_3\})_4(\mu_4\text{-O})]_2[\alpha\text{-SiMo}_{12}\text{O}_{40}] \cdot 4\text{H}_2\text{O}$ (**2**), $[(\text{Au}\{\text{P}(m\text{-MePh})_3\})_4(\mu_4\text{-O})]_2[\alpha\text{-SiW}_{12}\text{O}_{40}]$ (**3**) and $[(\text{Au}\{\text{P}(m\text{-MePh})_3\})_4(\mu_4\text{-O})]_2[\alpha\text{-SiMo}_{12}\text{O}_{40}]$ (**4**). The reaction of the less-acidic Keggin POM, *i.e.*, $\text{Na}_3[\alpha\text{-PW}_{12}\text{O}_{40}] \cdot 9\text{H}_2\text{O}$, with the monomeric gold(I) precursor complex containing para-methyl group substituted triarylphosphane ligands has formed the intercluster compound of heptaphosphanegold(I) cluster cation, *i.e.*, $[(\text{Au}\{\text{P}(p\text{-MePh})_3\})_4(\mu_4\text{-O})] \{(\text{Au}\{\text{P}(p\text{-MePh})_3\})_3(\mu_3\text{-O})\} [\alpha\text{-PW}_{12}\text{O}_{40}]$ (**5**). This work suggests the synthetic routes of a variety of oxygen-centered phosphanegold(I) clusters formed by a combination of the monomeric phosphanegold(I) carboxylate and the various POMs such as Dawson

and Anderson POMs, lacunary species of Keggin and Dawson POMs, and so on. Research in this direction is in progress.

Acknowledgments

This work was supported by JSPS KAKENHI grant number 22550065 and also by the Strategic Research Base Development Program for Private Universities of the Ministry of Education, Culture, Sports, Science and Technology of Japan.

Author Contributions

The synthesis and characterization of **1–4** were performed by Takuya Yoshida. The synthesis and characterization of **5** were performed by Yuta Yasuda. Characterization of these compounds were assisted by Eri Nagashima and Hidekazu Arai. Full research assistance and methodology were provided by Satoshi Matsunaga and Kenji Nomiya. The preparation of the manuscript was made by all the authors.

Conflicts of Interest

The authors declare no conflict of interest.

References

1. Pope, M.T.; Müller, A. Polyoxometalate Chemistry: An Old Field with New Dimensions in Several Disciplines. *Angew. Chem. Int. Ed. Engl.* **1991**, *30*, 34–48.
2. Hill, C.L.; Prosser-McCartha, C.M. Homogeneous catalysis by transition metal oxygen anion clusters. *Coord. Chem. Rev.* **1995**, *143*, 407–455.
3. Okuhara, T.; Mizuno, N.; Misono, M. Catalytic Chemistry of Heteropoly Compounds. *Adv. Catal.* **1996**, *41*, 113–252.
4. Proust, A.; Thouvenot, R.; Gouzerh, P. Functionalization of polyoxometalates: Towards advanced applications in catalysis and materials science. *Chem. Commun.* **2008**, 1837–1852.
5. Long, D.-L.; Tsunashima, R.; Cronin, L. Polyoxometalates: Building Blocks for Functional Nanoscale Systems. *Angew. Chem. Int. Ed.* **2010**, *49*, 1736–1758.
6. Nomiya, K.; Sakai, Y.; Matsunaga, S. Chemistry of Group IV Metal Ion-Containing Polyoxometalates. *Eur. J. Inorg. Chem.* **2011**, *2011*, 179–196.
7. Schulz-Dobrick, M.; Jansen, M. Supramolecular Intercluster Compounds Consisting of Gold Clusters and Keggin Anions. *Eur. J. Inorg. Chem.* **2006**, *2006*, 4498–4502.
8. Schulz-Dobrick, M.; Jansen, M. Synthesis and Characterization of Intercluster Compounds Consisting of Various Gold Clusters and Differently Charged Keggin Anions. *Z. Anorg. Allg. Chem.* **2008**, *634*, 2880–2884.
9. Noguchi, R.; Hara, A.; Sugie, A.; Nomiya, K. Synthesis of novel gold(I) complexes derived by AgCl-elimination between [AuCl(PPh₃)] and silver(I) heterocyclic carboxylates, and their antimicrobial activities. Molecular structure of [Au(*R,S*-Hpyrrld)(PPh₃)] (H₂pyrrld = 2-pyrrolidone-5-carboxylic acid. *Inorg. Chem. Commun.* **2006**, *9*, 355–359.

10. Nomiya, K.; Yoshida, T.; Sakai, Y.; Nanba, A.; Tsuruta, S. Intercluster Compound between a Tetrakis{triphenylphosphinegold(I)}oxonium Cation and a Keggin Polyoxometalate (POM): Formation during the Course of Carboxylate Elimination of a Monomeric Triphenylphosphinegold(I) Carboxylate in the Presence of POMs. *Inorg. Chem.* **2010**, *49*, 8247–8254.
11. Yoshida, T.; Nomiya, K.; Matsunaga, S. Novel intercluster compound between a heptakis{triphenylphosphinegold(I)}dioxonium cation and an α -Keggin polyoxometalate anion. *Dalton Trans.* **2012**, *41*, 10085–10090.
12. Yoshida, T.; Matsunaga, S.; Nomiya, K. Two types of tetranuclear phosphane-gold(I) cations as dimers of dinuclear units, $[\{(\text{Au}\{\text{P}(p\text{-RPh})_3\})_2(\mu\text{-OH})\}_2]^{2+}$ ($R = \text{Me}, \text{F}$), synthesized by polyoxometalate-mediated clusterization. *Dalton Trans.* **2013**, *42*, 11418–11425.
13. Yoshida, T.; Matsunaga, S.; Nomiya, K. Novel Intercluster Compounds Composed of a Tetra{phosphane-gold(I)}oxonium Cation and an α -Keggin Polyoxometalate Anion Linked by Three Monomeric Phosphane-gold(I) Units. *Chem. Lett.* **2013**, *42*, 1487–1489.
14. Yoshida, T.; Yasuda, Y.; Nagashima, E.; Arai, H.; Matsunaga, S.; Nomiya, K. Template Effects of Polyoxometalate (POM) in the Formation of Dimer-of-Dinuclear Phosphane-gold(I) Clusters by POM-Mediated Clusterization. Kanagawa university, Hiratsuka, Japan, Unpublished work, 2014.
15. Schmidbaur, H. Ludwig Mond Lecture. High-carat gold compounds. *Chem. Soc. Rev.* **1995**, *24*, 391–400.
16. Schmidbaur, H.; Schier, A. A briefing on aurophilicity. *Chem. Soc. Rev.* **2008**, *37*, 1931–1951.
17. Gimeno, M.C.; Laguna, A. Chalcogenide centred gold complexes. *Chem. Soc. Rev.* **2008**, *37*, 1951–1966.
18. Nesmeyanov, A.N.; Perevalova, E.G.; Struchkov, Y.T.; Antipin, M.Y.; Grandberg, K.I.; Dyadchenko, V.P. Tris{triphenylphosphinegold}oxonium salts. *J. Organomet. Chem.* **1980**, *201*, 343–349.
19. Yang, Y.; Ramamoorthy, V.; Sharp, P.R. Late transition metal oxo and imido complexes. 11. Gold(I) oxo complexes. *Inorg. Chem.* **1993**, *32*, 1946–1950.
20. Angermaier, K.; Schmidbaur, H. A New Structural Motif of Gold Clustering at Oxide Centers in the Dication $[\text{Au}_6\text{O}_2(\text{PMe}_3)_6]^{2+}$. *Inorg. Chem.* **1994**, *33*, 2069–2070.
21. Chung, S.-C.; Krüger, S.; Schmidbaur, H.; Rösch, N. A Density Functional Study of Trigold Oxonium Complexes and of Their Dimerization. *Inorg. Chem.* **1996**, *35*, 5387–5392.
22. Rocchiccioli-Deltcheff, C.; Fournier, M.; Franck, R.; Thouvenot, R. Vibrational Investigations of Polyoxometalates. 2. Evidence for Anion–Anion Interactions in Molybdenum(VI) and Tungsten(VI) Compounds Related to the Keggin Structure. *Inorg. Chem.* **1983**, *22*, 207–216.
23. Wells, A.F. *Structural Inorganic Chemistry*, 4th ed.; Clarendon Press: Oxford, UK, 1975; p. 1020.
24. Bondi, A. van der Waals Volumes and Radii. *J. Phys. Chem.* **1964**, *68*, 441–451.
25. North, E.O.; Haney, W. Silicomolybdic Acid. *Inorg. Synth.* **1939**, *1*, 127–129.
26. Tézé, A.; Hervé, G. α -, β -, and γ -Dodecatungstosilicic Acids: Isomers and Related Lacunary Compounds. *Inorg. Synth.* **1990**, *27*, 85–96.
27. Aoki, S.; Kurashina, T.; Kasahara, Y.; Nishijima, T.; Nomiya, K. Polyoxometalate (POM)-based, multi-functional, inorganic-organic, hybrid compounds: Syntheses and molecular structures of silanol- and/or siloxane bond-containing species grafted on mono- and tri-lacunary Keggin POMs. *Dalton Trans.* **2011**, *40*, 1243–1253.

28. Sheldrick, G.M. A short history of SHELX. *Acta Crystallogr.* **2008**, *64*, 112–122.
29. Sheldrick, G.M. *SADABS, Program for Area Detector Adsorption Correction*; University of Göttingen: Göttingen, Germany, 1997.
30. Spek, A.L. PLATON, an Integrated Tool for the Analysis of the Results of a Single Crystal Structure Determination. *Acta Crystallogr.* **1990**, *46*, c34.
31. Momma, K.; Izumi, F. VESTA 3 for three-dimensional visualization of crystal, volumetric and morphology data. *J. Appl. Crystallogr.* **2011**, *44*, 1272–1276.

© 2014 by the authors; licensee MDPI, Basel, Switzerland. This article is an open access article distributed under the terms and conditions of the Creative Commons Attribution license (<http://creativecommons.org/licenses/by/4.0/>).